

Recovery from Chronic Spinal Cord Contusion after Nogo Receptor Intervention

Xingxing Wang,¹ Philip Duffy,¹ Aaron W. McGee,^{1,2} Omar Hasan,¹ Grahame Gould,¹ Nathan Tu,¹ Noam Y. Harel,¹ Yiyun Huang,³ Richard E. Carson,³ David Weinzimmer,³ Jim Ropchan,³ Larry I. Benowitz,⁴ William B. J. Cafferty,¹ and Stephen M. Strittmatter¹

Objective: Several interventions promote axonal growth and functional recovery when initiated shortly after central nervous system injury, including blockade of myelin-derived inhibitors with soluble Nogo receptor (NgR1, RTN4R) decoy protein. We examined the efficacy of this intervention in the much more prevalent and refractory condition of chronic spinal cord injury.

Methods: We eliminated the NgR1 pathway genetically in mice by conditional gene targeting starting 8 weeks after spinal hemisection injury and monitored locomotion in the open field and by video kinematics over the ensuing 4 months. In a separate pharmacological experiment, intrathecal NgR1 decoy protein administration was initiated 3 months after spinal cord contusion injury. Locomotion and raphespinal axon growth were assessed during 3 months of treatment between 4 and 6 months after contusion injury.

Results: Conditional deletion of NgR1 in the chronic state results in gradual improvement of motor function accompanied by increased density of raphespinal axons in the caudal spinal cord. In chronic rat spinal contusion, NgR1 decoy treatment from 4 to 6 months after injury results in 29% (10 of 35) of rats recovering weight-bearing status compared to 0% (0 of 29) of control rats ($p < 0.05$). Open field Basso, Beattie, and Bresnahan locomotor scores showed a significant improvement in the NgR-treated group relative to the control group ($p < 0.005$, repeated measures analysis of variance). An increase in raphespinal axon density caudal to the injury is detected in NgR1 decoy-treated animals by immunohistology and by positron emission tomography using a serotonin reuptake ligand.

Interpretation: Antagonizing myelin-derived inhibitors signaling with NgR1 decoy augments recovery from chronic spinal cord injury.

ANN NEUROL 2011;70:805–821

Spinal cord injury (SCI) causes profound and persistent neurological deficits, many of which result from the interruption of axonal connectivity. A small number of compounds have been identified that when administered within the first few days subsequent to SCI either limit the extent of cell death following injury to lessen the resulting deficit, or promote the regrowth and/or collateral sprouting of axons to restore functional connectivity, or both.^{1,2} The regrowth of axons that bridge the lesion and the collateral sprouting of injured as well as

uninjured fibers rostral and caudal to the lesion play critical roles in determining the extent of neurological recovery.^{3,4} Recent studies have emphasized a tight correlation of sprouting with functional recovery even when frank regeneration is absent.^{5–8} Clinical trials are now testing the efficacy of several of these compounds in acute SCI.¹

Because SCI frequently occurs in young adults, and improved supportive care has dramatically increased life expectancy, the prevalence of chronic SCI is more than 20× the annual incidence of acute SCI.⁹ Neuroprotective

View this article online at wileyonlinelibrary.com. DOI: 10.1002/ana.22527

Received Mar 29, 2011, and in revised form Jun 1, 2011. Accepted for publication Jun 17, 2011.

Address correspondence to Dr Strittmatter, Yale University School of Medicine, Program in Cellular Neuroscience, Neurodegeneration, and Repair, P. O. Box 9812, New Haven, CT 06536-0812. E-mail: stephen.strittmatter@yale.edu

From the ¹Cellular Neuroscience, Neurodegeneration, and Repair Program, and Departments of Neurology and Neurobiology, Yale School of Medicine, New Haven, CT; ²Saban Research Institute, Children's Hospital Los Angeles, Keck School of Medicine, University of Southern California, Los Angeles, CA; ³Positron Emission Tomography Center, Department of Diagnostic Radiology, Yale School of Medicine, New Haven, CT; and ⁴Children's Hospital, Harvard Medical School, Boston, MA.

Additional supporting information can be found in the online version of this article.

strategies cannot benefit pre-existing chronic SCI, and strategies that promote axonal growth have shown efficacy only when administered shortly after injury. Thus, the prevailing model posits that the benefit of promoting axonal extension and collateral sprouting by blocking extrinsic inhibitors or enhancing intrinsic activators is restricted to the acute stage of injury following trauma, when axons are predicted to exhibit the highest potential for anatomical plasticity.¹⁰ However, a recent study demonstrated that extensive regrowth of injured axons across the lesion site can be induced long after injury.¹⁰ This approach required a combination of peripheral nerve injury, viral injection, and cell transplantation. Unfortunately, and perhaps unexpectedly, this regrowth did not result in any functional benefit. Thus, axons in the chronic stage postinjury did regrow, but the extension of severed axons alone is insufficient to restore central nervous system (CNS) function.¹⁰ Alternative cell-based multimodal therapies that include a component for blocking extrinsic inhibitors have also shown some success in specific chronic CNS injury models.^{11,12} However, pharmacological therapy for axonal growth with improved function in chronic SCI remains an unattained goal.

Myelin limits axonal growth and neurological recovery after SCI.² Among the inhibitory myelin proteins are Nogo-A (Rtn4A), myelin-associated glycoprotein (MAG, Siglec-4), and oligodendrocyte myelin glycoprotein (OMgp). Each exhibits affinity for the Nogo-66 receptor (NgR1, Rtn4R), a protein detectable on axons.¹³ The Nogo mutant phenotype has been controversial, and depends on the strain background¹⁴ and the lesion model¹⁵ as well as the specific allele,^{7,15–17} which is crucial to avoid chronic compensatory effects from other loci (Cafferty and Strittmatter, unpublished observations). For those models with a detectable Nogo-A phenotype, combined deletion of Nogo-A, MAG, and OMgp allows substantial recovery from spinal cord trauma, greater than deletion of Nogo-A alone and much greater than deletion of MAG and OMgp.^{7,14,15,18,19} For the receptor, constitutive deletion of NgR1 expression allows enhanced recovery after SCI or stroke, and permits sprouting and regenerative growth of raphespinal and rubrospinal axons.^{20,21} Sprouting, but not regeneration, of corticospinal fibers is observed.^{15,20–22} The Nogo, MAG, and OMgp ligands also bind paired-immunoglobulinlike receptor B (PirB) to inhibit axonal growth in vitro.²³ However, PirB mutant mice do not display improved recovery from CNS injury in any model yet tested.^{24,25}

The Nogo/NgR1 pathway has been targeted pharmacologically in acute and subacute CNS injury models by various methods. Anti-Nogo-A antibodies bind 1

myelin-associated inhibitory ligand (Nogo-A) and improve recovery when administered to rodents with spinal hemisection or stroke within 1 week of injury.^{26–28} Similar humanized versions of these antibodies are now completing phase 1 clinical trials.²⁹ An antagonist peptide, NEP1-40, selectively blocks Nogo-66 binding to NgR1 and promotes recovery from dorsal hemisection of thoracic spinal cord,^{30,31} lateral hemisection of cervical cord,³² and stroke.^{33,34} One NEP1-40 study observed only slight increase in sprouting and inconsistent behavioral improvements.³⁵ Greatest benefit is obtained by neutralization of all 3 myelin inhibitors with a soluble truncated NgR1 fusion protein, NgR1(310)ecto-Fc.³⁶ Infusing this NgR1 decoy protein into the CNS within a week of spinal cord dorsal hemisection, stroke, spinal cord contusion, or dorsal rhizotomy increases axonal growth responses and improves behavioral recovery.^{21,37–39} Downstream of NgR1, RhoA and ROCKII mediate myelin inhibition of axonal growth, and an RhoA inhibitor, ROCK inhibition, and *ROCKII* gene deletion all promote functional recovery after acute SCI.^{40–44} Critically, none of these interventions, nor any other pharmacological therapy to promote anatomical repair, has been reported to support neurological improvement when administered in the chronic stage postinjury after endogenous tissue responses have stabilized and the natural history is static.

We reasoned that because many axonal tracts and intrinsic spinal circuits remain intact in regions proximal and circumferential to SCI sites and are continually exposed to myelin and myelin debris, blockade of myelin inhibitors long after spinal injury might stimulate axonal growth and recovery. We utilized a drug-regulated conditional deletion of NgR1 and a pharmacological treatment with an NgR-Fc decoy protein, AA-NgR(310)ecto-Fc, to test this hypothesis. Here, we provide evidence that blockade of myelin inhibition allows raphespinal axon growth and enhances recovery in chronic SCI. In addition, we describe a clinically adaptable in vivo imaging method to monitor raphespinal axon growth stimulated by NgR decoy protein following chronic spinal contusion injury. Together, these data support a role for pharmacological interventions targeting myelin-associated inhibitors and their receptors as a treatment for chronic SCI.

Materials and Methods

Gene Targeting and Mouse Strains

The multiple cloning site of pBluescriptII-KS(+) was replaced with a combination of unique restriction sites to facilitate the sequential construction of the targeting construct. The complete plasmid comprises (in order) a 6.6Kb flanking arm of genomic

sequence 5' to a loxP site introduced at a Xho-I restriction site proximal to the 5' end of exon 2 of NgR1, a pGK-NEO cassette flanked by FRT sequences approximately 500nt 3' to the predicted end of the NgR1 mRNA, a second loxP site followed by the 86nt preceding the splice acceptor sequence and the first 12nt of exon 2 fused in-frame with enhanced green fluorescent protein (eGFP), including an SV-40 polyadenylation sequence, a 4Kb flanking arm of genomic sequence, and a negative selection cassette containing herpes simplex virus-thymidine kinase. The plasmid containing the targeting construct was linearized at a unique Sfi-I site and electroporated into embryonic stem (ES) cells. ES cells were selected using G418 and FIAU. Chimeric mice were generated and crossed first onto the C57BL/6J strain and then a C57BL/6J strain expressing the Flp recombinase ubiquitously (Flp deleter strain). Progeny of this cross was screened by polymerase chain reaction to confirm the removal of the pGK-NEO cassette.

The estrogen-regulated ubiquitous cre recombinase mouse strain pActin-ER-Cre (B6.Cg-Tg[CAG-cre/Esr1]5Amc/J)⁴⁵ was obtained from Jackson Laboratories (Bar Harbor, ME). The constitutive mouse strain pActin-Cre (Tg[CAG-cre]1Nagy) was provided by the Yale Animal Genomics Services Center. Tamoxifen was solubilized in corn oil to 10mg/ml by heating to 37°C and sonicating repeatedly. The drug was administered at a dose of 100mg/kg by intraperitoneal injection for 3 consecutive days. Mice were backcrossed to C57Bl6J for >6 generations.

Southern Blot

Genomic DNA was prepared from cerebral cortex and hippocampus. Genomic DNA was digested with Hind-III, separated by electrophoresis, and blotted onto nylon membranes (BrightStar-Plus; Ambion, Austin, TX). The NgR1 probe was amplified with the following primers: NR1 forward, 5'-TTC AGA TGT GTG GTT TTG GTG ACC-3' (beginning at nt 221 5' to the beginning of exon 2), and NR1 reverse: 5'-GAA GGT GAG GAG GAA GAG AGG GAG-3' (ending at nt 721 5' to the beginning of exon 2). The GFP probe corresponded to 400nt of eGFP amplified with GFP forward 5'-GGC GAG GGC GAT GCC ACC TAC GGC-3' (beginning at nt 100 after the start ATG), and GFP reverse 5'-GCG GAT CTT GAA GTT CAC CTT GAT GCC-3' (ending at nt 507 after the start ATG). The purified probe template was biotinylated with the BrightStar Psoralen-Biotin Kit (Ambion). Blots were hybridized overnight with denatured probe at 68°C. After washing, bound probe was detected with the BrightStar Biotect Kit and autoradiography film.

Northern Blot

Cerebral cortex and hippocampus from 1 hemisphere were homogenized in 20 volumes (wt/vol) of Trizol Reagent (Invitrogen, Carlsbad, CA), aliquoted, frozen in liquid nitrogen, and stored at -80°C. Thirty micrograms of total RNA was isolated and then separated on a 1% formaldehyde-agarose gel and blotted to nylon membrane (BrightStar-Plus, Ambion). Probes were prepared with the BrightStar psoralen-biotin nonisotopic labeling kit (Ambion) as described for Southern blotting (above).

The NgR1 probe was prepared by first amplifying the cDNA sequence corresponding to the ~600nt carboxyl-terminal half of NgR1 with the following primers: NR1 forward, 5'-CAG TAC CTG CGA CTC AAT GAC AAC CCC-3' (beginning at nt 757 relative to the start ATG), and NR1 reverse: 5'-CTT CCG GGA ACA ACC TGG CCT CC-3' (ending at nt 1,266 relative to the start ATG). The GFP probe is identical to the probe used for Southern blotting. After hybridization, bound probe was detected with the BrightStar Biotect Kit.

Immunoblots

Cerebral cortex and hippocampus were homogenized in 20 volumes (wt/vol) of 100mM NaCl, 10mM Tris-Cl pH 7.4, and Triton X-100 and sodium dodecyl sulfate were added to 1% and 0.5%, respectively. After centrifugation at 20,000 × *g* for 15 minutes, the supernatant was collected and assessed by immunoblot with antibodies directed against either NgR1 (goat antimouse NgR1; R&D Systems, Minneapolis, MN) or GFP (rabbit anti-GFP; Sigma, St Louis, MO). Immunoreactivity was detected with horseradish peroxidase-coupled secondary antibodies (Jackson ImmunoResearch, West Grove, PA) and chemiluminescence (Pierce, Rockford, IL).

Optic Nerve Crush Injury and Regeneration

Cohorts of mice were administered tamoxifen 7 to 9 days prior to injury, as described above. To crush the optic nerve, mice at 8 to 10 weeks of age were anesthetized with an intraperitoneal injection of ketamine (100mg/kg) and xylazine (10mg/kg) and placed in a stereotactic apparatus. Topical 2% lidocaine anesthetic was applied to the eyeball. The right optic nerve was exposed intraorbitally with care taken to avoid damage to the ophthalmic artery. The nerve was injured by crushing with a jeweler's forceps (Dumont #5; Fine Science Tools, Foster City, CA) for 10 seconds at a location 1mm posterior to the eyeball. Two weeks thereafter, animals were anesthetized with an overdose of anesthetic and perfused transcardially with phosphate-buffered saline (PBS) followed by 4% paraformaldehyde. The optic nerves and retinas were dissected and postfixed in 4% paraformaldehyde for 48 hours. The specimens were then transferred to 30% sucrose for cryoprotection, embedded in optimal cutting temperature medium, and cryosectioned in the longitudinal plane at 16µm thickness. The sections were stained with anti-GAP-43 antibody (1:1,000) followed by a fluorescent-tagged donkey antisheep (immunoglobulin G [IgG]) secondary antibody. Four longitudinal sections of optic nerve were selected from each animal. The number of GAP-43-positive axons was counted at 0.5mm and 1mm distal to the lesion site. The total number of regenerating axons was calculated from these counts.⁴⁶ The retina was also examined for ganglion cell survival using anti-βIII tubulin antibody. No differences were detected between different nerve crush groups (data not shown).

Chronic Thoracic Dorsal Hemisection Injury

Dorsal hemisections were performed on mice by a surgeon blind to the cre transgene genotype using methods and postoperative care as described previously.^{7,18} All mice had Basso

Mouse Scale (BMS) scores of ≤ 4 at 75 days postinjury prior to tamoxifen treatment by the method described above.

Chronic Rat Spinal Contusion Injury with Prolonged Intracerebroventricular Therapy

Female Sprague-Dawley rats (250–270g, 11–12 weeks of age, $n = 70$) were anesthetized with intraperitoneal injection of ketamine (60mg/kg) and xylazine (10mg/kg). A laminectomy was conducted at the caudal portion of T6 and all of T7 spinal levels. A T7 moderate contusion injury (10g, 25mm) was produced with the MASCIS impactor.^{37,47,48} After the contusion, locomotor performance was assessed at 1-week intervals using the Basso, Beattie, and Bresnahan (BBB) score in the open field. Locomotor performance stabilized at a score of 8 by 7 weeks after injury.

An intracerebroventricular cannula was used for AA-NgR(310)ecto-Fc therapy. To avoid any confounding unfavorable effect of the cannula implantation procedure on locomotor scores, a cannula (Alzet Brain Infusion Kit II; ALZA Corporation, Mountain View, CA) was implanted into the right lateral ventricle at 10 weeks after contusion injury as described previously.^{21,49} Briefly, the scalp was opened, a burr hole was drilled through the skull, and a cannula was introduced into the right lateral ventricle at stereotaxic coordinates 0.6mm posterior and 1.2mm lateral to bregma and 4.0mm deep relative to the pial surface. The cannula was connected to an osmotic minipump containing PBS placed subcutaneously over the scapulae. The cannula was fixed in place with cyanoacrylate, and the skin was sutured.

Two weeks after cannula implantation (12 weeks after contusion injury), the rats were reanesthetized, and the minipumps were replaced with new osmotic minipumps (ALZA Corporation) connected to the same cannula. These pumps delivered 2.5 μ l/h for 28 days and were filled with 2.25mg AA-NgR(310)ecto-Fc (0.29 mg/kg/day) or 2.25mg IgG from rat serum (#14131, 50mg, Sigma) in 2ml PBS. A total of 64 rats survived from contusion injury to 12 weeks and were entered with into the treatment randomization. Rats were randomly assigned to 1 of the 2 groups, and the surgeon was unaware of the assignment. The duration of treatment was 12 weeks. A new osmotic minipump filled with the same amount of AA-NgR(310)ecto-Fc or rat IgG was switched every 4 weeks.

AA-NgR(310)ecto-Fc Protein

Purified rat protein was produced in Chinese hamster ovary cells and purified as described previously³⁸ with 1 modification. Because the wild fusion protein exhibits a high percentage of disulfide bond heterogeneity, a variant was produced in which the 2 Cys residues at position 266 and 309 of the full-length NgR1 were changed to Ala. This AA variant is homogenous with respect to disulfide bonding and is fully active in vitro.⁵⁰

Behavioral Testing

For mouse behavioral observation, the BMS locomotor scale was used.⁵¹ For rat behavioral testing, the BBB locomotor scale was used.^{47,52} All behavioral tests were performed by 2

researchers unaware of the genotype of the mice or of the identity of the compound in the minipump. Observations were made once per week. Grip strength was measured using a Columbus Instruments (Columbus, OH) force meter for a random subset of animals. Each rat was tested 3 \times for each limb, and the data were averaged.

Limb Kinematics

One week before initiation of treatment (tamoxifen or AA-NgR[310]ecto-Fc protein), and several months later near the end of treatment, mice or rats were video-recorded while locomoting to the end of a 1m Plexiglas track. Prior to video monitoring, reflective markers (B&L Engineering, Santa Ana, CA) were attached using nontoxic glue bilaterally to the iliac crest, the head of the humerus, the greater trochanter of the knee, the lateral malleolus, the fifth metatarsal, and the third toe. Recordings were made from 4 synchronized cameras at 100Hz (Basler Vision Technologies, Ahrensburg, Germany) placed at approximately 45° and 135° relative to the position of the track. We utilized the SIMI motion-capture software (SIMI Reality Motion Systems, Unterschleissheim, Germany) to obtain 3-dimensional coordinates of the markers during locomotion. We modeled the hind limb as an interconnected chain of rigid segments. We then extrapolated multiple gait parameters from recordings containing at least 3 consecutive step cycles.

Data was exported using the SIMI motion-capture software numerically in Excel (Microsoft Corporation, Redmond, WA) spreadsheets and as individual frame-by-frame images of gait cycles of each animal. We analyzed the position of the toe relative to distance traveled in the y (anterior–posterior) plane and z plane (superior–inferior), after normalizing the position of the toe relative to a fixed iliac crest (rat) or hip (mouse) to analyze the swing phase of the gait cycle. Additional measures were the angle of the ankle joint and the absolute velocity of the foot as functions of time. The gait cycle was defined as a single attempted forward excursion by the hindlimb, as many of the animals were unable to step due to the nature of the injury. Frame-by-frame images were analyzed using ImageJ (National Institutes of Health, Bethesda, MD) and Illustrator (Adobe Systems, San Jose, CA).

Histology and Analysis

Animals were perfused transcardially with PBS, followed by a 4% paraformaldehyde/PBS solution. The spinal cord 10mm rostral to and 10mm caudal to the lesion center was embedded in a glutaraldehyde–polymerized albumin matrix and cut parasagittally in the thickness of 40 μ m on a vibratome. Transverse sections (40 μ m) were collected from the spinal cord 11 to 16mm rostral to and 11 to 16mm caudal to the lesion center.^{15,18,20,30,31,37,38,53,54}

Sagittal sections of thoracic spinal cord were incubated with anti-5-hydroxytryptamine (anti-5HT) antibody (1:10,000; Immunostar, Hudson, WI) and then with Alexa Fluor 568-labeled secondary antibody (Invitrogen) to detect raphespinal fibers.^{15,18,20,30,31,37,38,53,54} Transverse sections 11 to 16mm caudal to the lesion center were incubated with anti-5HT

antibody or anti-serotonin transporter antibody (1:10,000 or 1:1,000; Immunostar) and were visualized with appropriate secondary antibody conjugated to Alexa Fluor 568 (Invitrogen).

Image analysis was performed with the National Institutes of Health's ImageJ version 1.62, as described previously.^{15,18,20,30,31,37,38,53,54} For analysis of serotonin innervation, immunoreactive serotonin fibers in the ventral horn of transverse sections caudal to the lesion center were selected by thresholding; then the length of serotonin fiber per area was measured after using the skeletonize function. For camera lucida tracing of 5HT-immunoreactive fibers, 10 serial sections at 200 μ m intervals from each animal were photographed digitally, and fibers were traced on a computer using Adobe Photoshop 7.0 software (Adobe Systems, Mountain View, CA).

Positron Image Tomography with [¹¹C]AFM

Cohorts of injured rats were imaged twice, once at 12 weeks after spinal contusion prior to treatment, and again after 12 weeks of treatment. Uninjured control rats or complete transection rats were imaged once. Rats were anesthetized by isoflurane inhalation, and then 50 ± 30 MBq of [¹¹C]AFM ([¹¹C]-2-[2-(dimethylaminomethyl)phenylthio]-5-fluoromethylphenylamine) was administered in sterile saline by tail vein injection (injected mass: 0.12 ± 0.09 μ g). After injection, dynamic positron emission tomography (PET) images were acquired on a high-resolution research tomograph scanner for 2 hours, as described.^{55,56} Images were collected from 3 rats simultaneously in each imaging session, and radioactivity concentration was assessed in the spinal cord at the cervical and lumbar enlargements. A subset of rats was imaged twice with [¹¹C]AFM, once under baseline condition, and once after receiving citalopram, a serotonin transporter inhibitor (2mg/kg in saline) 15 minutes prior to the second [¹¹C]AFM PET scan to block specific binding sites. Nonspecific uptake (~30% of cervical uptake) detected in the presence of citalopram was subtracted from the total uptake, to assess [¹¹C]AFM specific binding signal.

Results

Conditional Gene Targeting of the *ngr1* Locus

To test definitively whether loss of NgR1 function in the chronically injured state might yield functional benefit, we generated a conditionally targeted NgR1 allele, *ngr1^{fllox}*, by flanking the second exon (containing the entire coding sequence for the mature protein) with *loxP* sites (Supplementary Fig S1). In mice harboring a transgene of cre recombinase (Cre) driven by the constitutive β -actin promoter, recombination of the NgR1 allele is essentially complete. To provide temporal control over deletion, we utilized a transgene with this promoter that drives expression of a fusion protein of Cre and a mutant version of the estrogen receptor (ER).⁴⁵ Tamoxifen treatment leads to highly efficient NgR1 gene rearrangement and near total loss of mRNA and protein in the adult CNS within 1 week (Fig 1A). Prior to recombination,

this allele expresses NgR1 protein at wild-type (WT) levels (see Fig 1A). After Cre-mediated recombination, this allele produces detectable GFP mRNA and protein. GFP expression levels are not sufficient to permit visualization of intrinsic GFP fluorescence but can be detected with signal amplification.

To assess the functional completeness of NgR1 loss following tamoxifen treatment, we employed an optic nerve regeneration model. Previous studies have demonstrated that expression of a dominant negative form of NgR1 in retinal ganglion cells with a recombinant virus yields a subtle axon regeneration phenotype that substantially synergizes with an enhancement of intrinsic growth potential by intraocular inflammation.⁴⁶ A constitutive null allele of *ngr1* has a stronger axonal regeneration phenotype after optic nerve crush that is clearly detectable without zymosan injection or lens injury (see Fig 1B-D). We examined whether the conditional deletion of *ngr1* would produce an axonal regeneration phenotype similar to the constitutive knockout. Axonal regeneration in *ngr1^{fllox/-}* mice carrying the Cre transgene and treated with tamoxifen 1 week prior to optic nerve crush resembles that in *ngr1^{-/-}* mice and is significantly ($p < 0.01$, analysis of variance [ANOVA]) greater than in WT mice. Axonal regeneration is not as complete in the conditional allele as the constitutive deletion; this is likely to reflect the 7-day pretreatment providing subtotal gene rearrangement (see Fig 1A). For *ngr1^{fllox/-}* mice without Cre/tamoxifen, axonal regeneration was not significantly different from the low WT levels (see Fig 1B, D). Thus, the conditional allele allows functional deletion of NgR1 in vivo by tamoxifen, and resembles the *ngr1* null axonal regeneration phenotype.

Functional Improvement and Raphespinal Growth after Genetic Deletion of NgR1 in Chronic Mouse SCI

Next, we utilized the conditional *ngr1* allele to assess recovery and axonal growth in the chronic postinjury state. Optic nerve regeneration is not a chronic injury model, as the vast majority of retinal ganglion cells die within 1 month of injury.^{57,58} Instead, we subjected *ngr1^{fllox/-}* and *ngr1^{fllox/fllox}* mice, of which 18 of 41 also carried the Cre/Esr1 transgene, to a spinal cord dorsal hemisection injury. Animals were then observed without intervention for 75 days, a duration greater than the time course of natural (limited) recovery (Fig 2A). At 75 days, prior to tamoxifen treatment when NgR1 expression is at WT levels, no differences in locomotor performance are detected between these genotypes (BMS = 2.95 ± 0.15 at 2 months in Fig 2B). All mice were treated with tamoxifen at 75 days postinjury. Over the ensuing 125

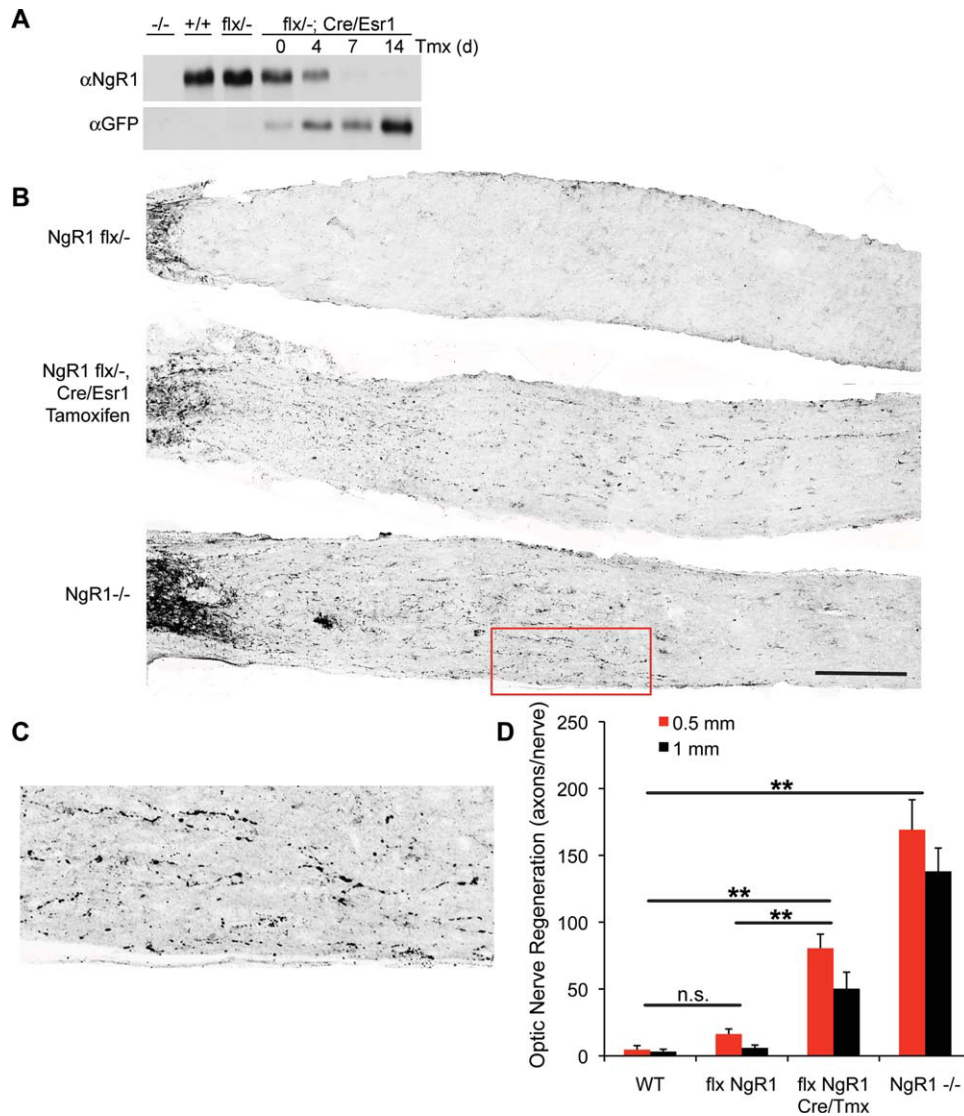


FIGURE 1: Recovery from chronic spinal cord injury deficits after NgR1 deletion. (A) Cre-mediated recombination from the pActin-Cre/Esr1 transgene abolishes expression of NgR1 following tamoxifen injection. Immunoblots are shown of brain lysate from mice transgenic for pActin-Cre/Esr1 at several time points after tamoxifen injection to activate the Cre fusion protein with antibodies directed against either NgR1 or green fluorescent protein (GFP). (B) Mice of the indicated genotypes underwent optic nerve crush injury at 10 to 12 weeks of age, and tissue was collected 14 days later for anti-GAP-43 immunohistology of injured fibers. The flx NgR1 mice carrying the cre/Esr1 transgene were treated with tamoxifen 1 week prior to injury. Intact fibers close to the eye are visible at the far left, and regeneration past the lesion is detected in the bottom 2 panels. Scale bar = 250 μ m. (C) Higher magnification view of the area boxed in red in B demonstrates regenerating fibers in NgR1 -/- mice. (D) The number of regenerating optic nerve fibers is presented as a function of distance central to the crush site and of genotype. Data are mean \pm standard error of the mean for 4 to 8 mice per group. ** $p < 0.01$, 1-way analysis of variance with pairwise post hoc Fisher least significant difference test (SPSS Inc., Chicago, IL). The indicated comparisons are valid at both the 0.5mm and the 1mm distances. n.s. = not significant; WT = wild type.

days, mice expressing ER-Cre, and therefore lacking NgR1 expression, exhibited improved open field BMS locomotion scores. Over this time frame, there was no significant improvement in the Cre-negative group (final BMS = 3.40 \pm 0.25) relative to the pretamoxifen performance (2 month BMS = 2.95 \pm 0.15). In contrast, the Cre-positive group improved significantly during the months post-tamoxifen (final BMS = 4.25 \pm 0.15, $p = 0.03$ by repeated measures ANOVA relative to Cre-nega-

tive, and $p < 0.01$ at 5–7 months relative to the pretamoxifen 2-month value). On the BMS scale, a score of 3, the average starting point for both groups, represents plantar placing and/or dorsal stepping, but no plantar stepping. In comparison, a score of 4 or 5 indicates occasional or regular plantar stepping with weight support. Thus, Cre-mediated deletion of NgR1 expression in the chronic stage postinjury enabled affected mice to improve stepping performance. This improvement after NgR1

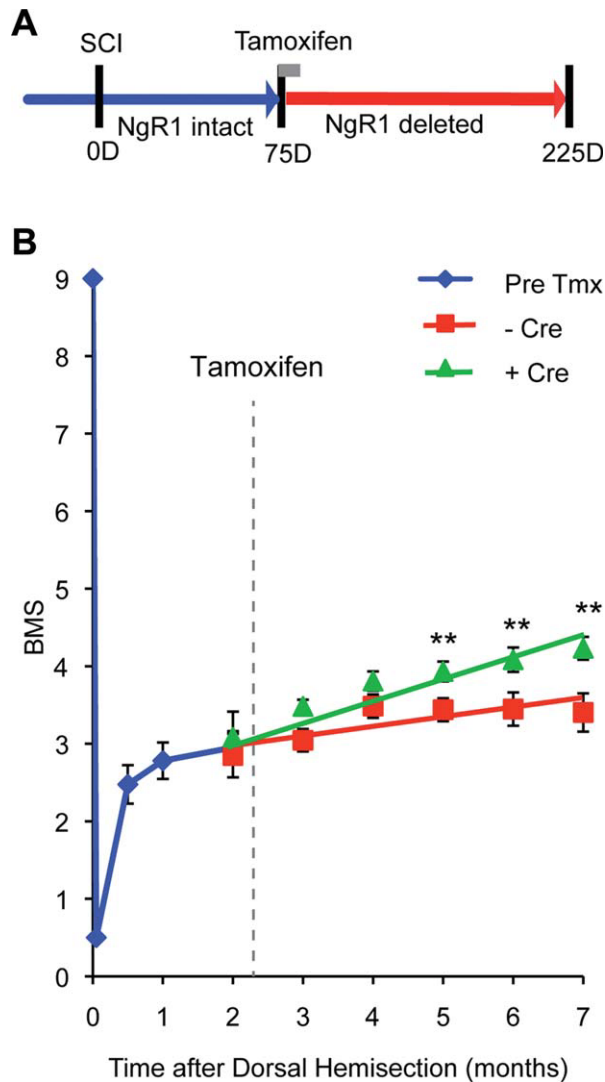


FIGURE 2: Recovery of locomotor function in chronic spinal cord hemisection by NgR1 deletion. (A) Schematic of mouse chronic spinal cord injury (SCI) experiment. All mice carried flx NgR1 alleles, but 1 group also carried the Cre/Esr1 transgene to allow tamoxifen-induced recombination (Cre-positive, $n = 23$), whereas the other group did not (Cre-negative, $n = 18$). Seventy-five days after SCI, mice received tamoxifen to abolish NgR1 expression. (B) The Basso Mouse Scale (BMS) score after the initiation of treatment is plotted. Recovery is greater in the Cre/Esr1 group: $p = 0.030$ by repeated measures analysis of variance (ANOVA) for the effect of Cre after tamoxifen treatment. Data are mean \pm standard error of the mean. $**p < 0.01$, 1-way ANOVA for the Cre-positive group relative to the pretamoxifen value by Fisher least significant difference test using SPSS software.

elimination was gradual over months, consistent with a chronic anatomical growth response as opposed to an acute biochemical event, which would have been evident within a week as NgR1 protein levels diminished.

Stepping performance was also assessed with high-speed video limb kinematics (Fig 3). Markers over each joint of both hindlimbs were tracked during unassisted

locomotion to provide the most functionally relevant performance. Uninjured mice exhibit robust step cycles, whereas 10 days after a total thoracic transection there is nearly complete paralysis. In mice with intact NgR1 expression, unassisted gait remained significantly impaired 6 to 7 months after dorsal hemisection, as expected for chronic postinjury mice. We focused on measures of the length and height of foot swing with each step cycle for chronic dorsal hemisection mice both before and after tamoxifen administration. Prior to tamoxifen treatment, the Cre-negative and Cre-positive groups displayed similar deficits. The anterior-posterior length of the foot swing relative to the hip was reduced by half compared to uninjured control mice. The vertical height of the foot cycle relative to the hip was also reduced by 50%. After tamoxifen treatment, these limb kinematic measurements in the Cre-negative group at 6 to 7 months were comparable to pretamoxifen 75-day postinjury values, revealing a stable gait impairment, with no change in the length or height of foot swing relative to the hip. In contrast, the average height and length of foot excursions in Cre-positive mice increased during the 5 months after tamoxifen treatment. These values represent statistically significant improvements ($p < 0.01$, 1-way ANOVA) relative to both the pretamoxifen values and to the Cre-negative group in which NgR1 expression was intact, but are significantly lower than the values for uninjured mice. Thus, foot movements remained restricted compared to uninjured mice, but improved after NgR1 deletion in chronically injured mice. The reproducibility of this phenotype is illustrated for 8 Cre-negative control and 8 Cre-positive mice (Supplementary Fig S2). Other measures of the gait cycle, including the foot velocity and the ankle angle, are different in the Cre-positive mice (Supplementary Fig S3). In particular, the ankle angle is more extended in the mice with NgR1 deletion (Cre-positive), and recovers after each step more quickly, than in the mice with NgR1 intact (Cre-negative).

Previously, we observed that following a dorsal hemisection SCI in mice with a constitutive deletion of NgR1, the density of fibers from the descending raphespinal serotonergic system increases caudal to the lesion.²⁰ In this study, at the conclusion of this extended observation period, we examined the distribution of serotonergic fibers in the spinal cords from both Cre-negative and Cre-positive mice. In both groups, raphespinal fibers were substantially depleted in the ventral horn of the lumbar caudal spinal cord relative to the cervical enlargement (Fig 4). Mice carrying the Cre transgene and thus lacking NgR1 beginning ~ 75 days after hemisection exhibit increased 5HT fiber density in the lumbar cord

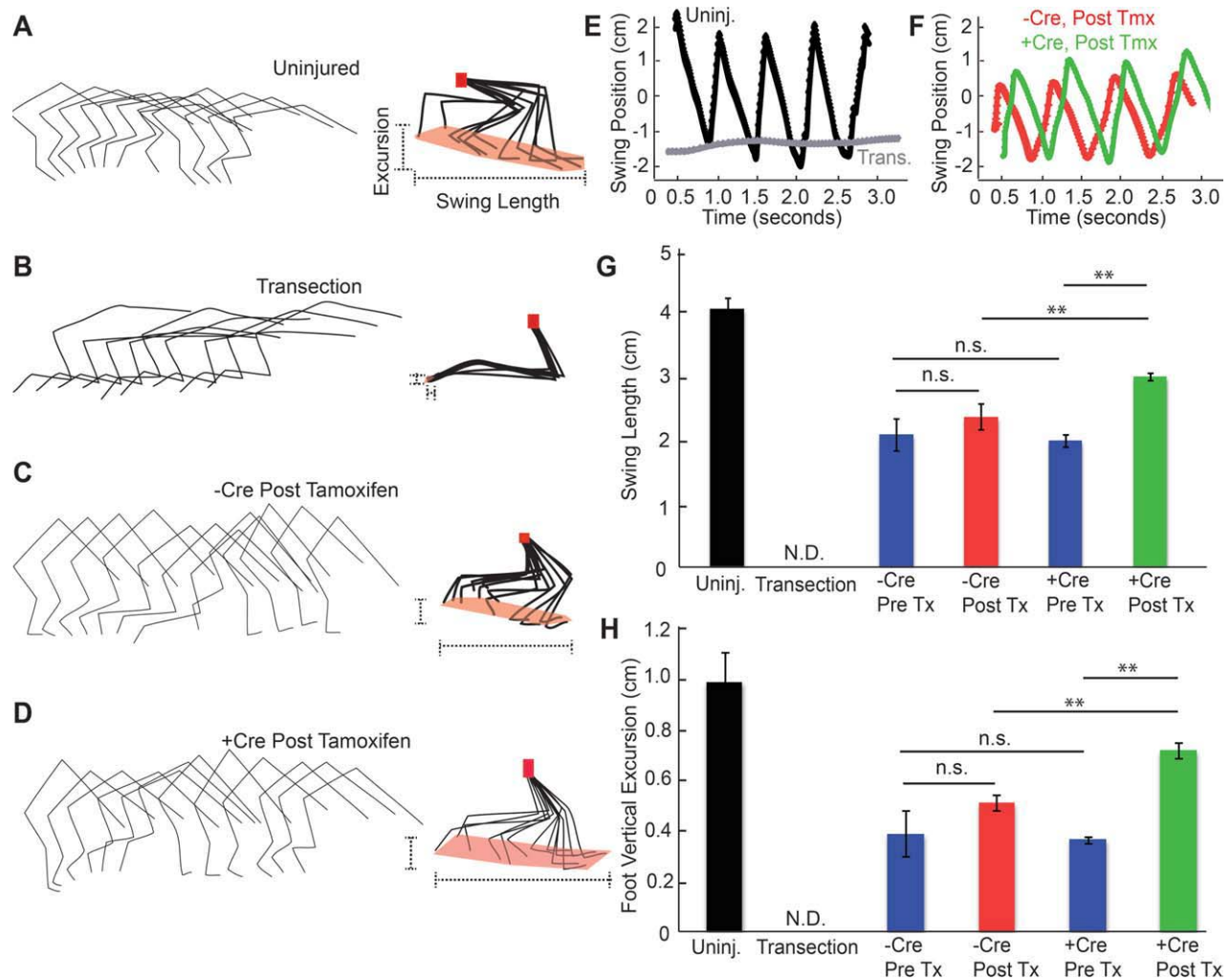


FIGURE 3: Kinematic analysis of hindlimb function after NgR1 deletion in chronic SCI. (A–D) Hindlimb kinematic analysis from individual mice with no injury (A), or a complete transection 7 days earlier (B) or dorsal hemisection 6 months earlier (C, D). The dorsal hemisection mice with flx NgR1 alleles were treated with tamoxifen 75 days after injury and either carried Cre transgene (D) or did not (C). Tracings of joint and limb position from 1 hindlimb during 1 gait cycle are shown for every 21st frame on the left. On the right, the foot, ankle, and knees have been normalized to the hip position (red dots). The extent of foot swing is highlighted (dotted lines). (E, F) The anterior–posterior position of the foot relative to the hip from 1 limb of each of the indicated groups as in A–D is plotted as a function of time. Gait cycles are reflected in sequential peaks. Uninj. = uninjured. (G) The length of the foot swing relative to the hip in the anterior–posterior dimension is shown for each group of mice. Mice were examined when uninjured, 1 week after complete spinal cord transection, or 10 to 35 weeks after dorsal hemisection injury. The Pre Tx groups were analyzed immediately before tamoxifen (10–11 weeks postinjury), and the Post Tx groups were analyzed 4 to 5 months after tamoxifen (30–35 weeks postinjury). Data are mean \pm standard error of the mean (SEM), $n = 46$ limbs for mice without Cre and $n = 36$ for mice with Cre transgene. $**p < 0.01$, 1-way analysis of variance (ANOVA) with pairwise post hoc Fisher least-significant difference test (SPSS). N.D. = not done; n.s. = not significant. (H) The vertical excursion of the foot relative to the hip is reported for the same groups of mice as in (G). Data are mean \pm SEM. $**p < 0.01$, 1-way ANOVA with pairwise post hoc analysis using SPSS software.

relative to Cre-negative controls (see Fig 4B, C). This increase may reflect axonal growth of spared fibers, long-distance growth of cut fibers, or both. Therefore, axonal growth in 1 or several tracts may contribute to the slow improvement in motor function observed in Cre-positive mice. There was a strong correlation of 5HT axon density with the parameters measured kinematically (see Fig 4D, E).

Improved Locomotion and Axon Growth after Treatment of Rat Chronic Spinal Contusion with AA-NgR(310)ecto-Fc

Based on these positive results with genetic perturbation of NgR1 expression in chronically injured mice, we next attempted a more clinically relevant pharmacological treatment of chronic spinal cord contusion in rats. A cohort of rats underwent midthoracic contusion; they

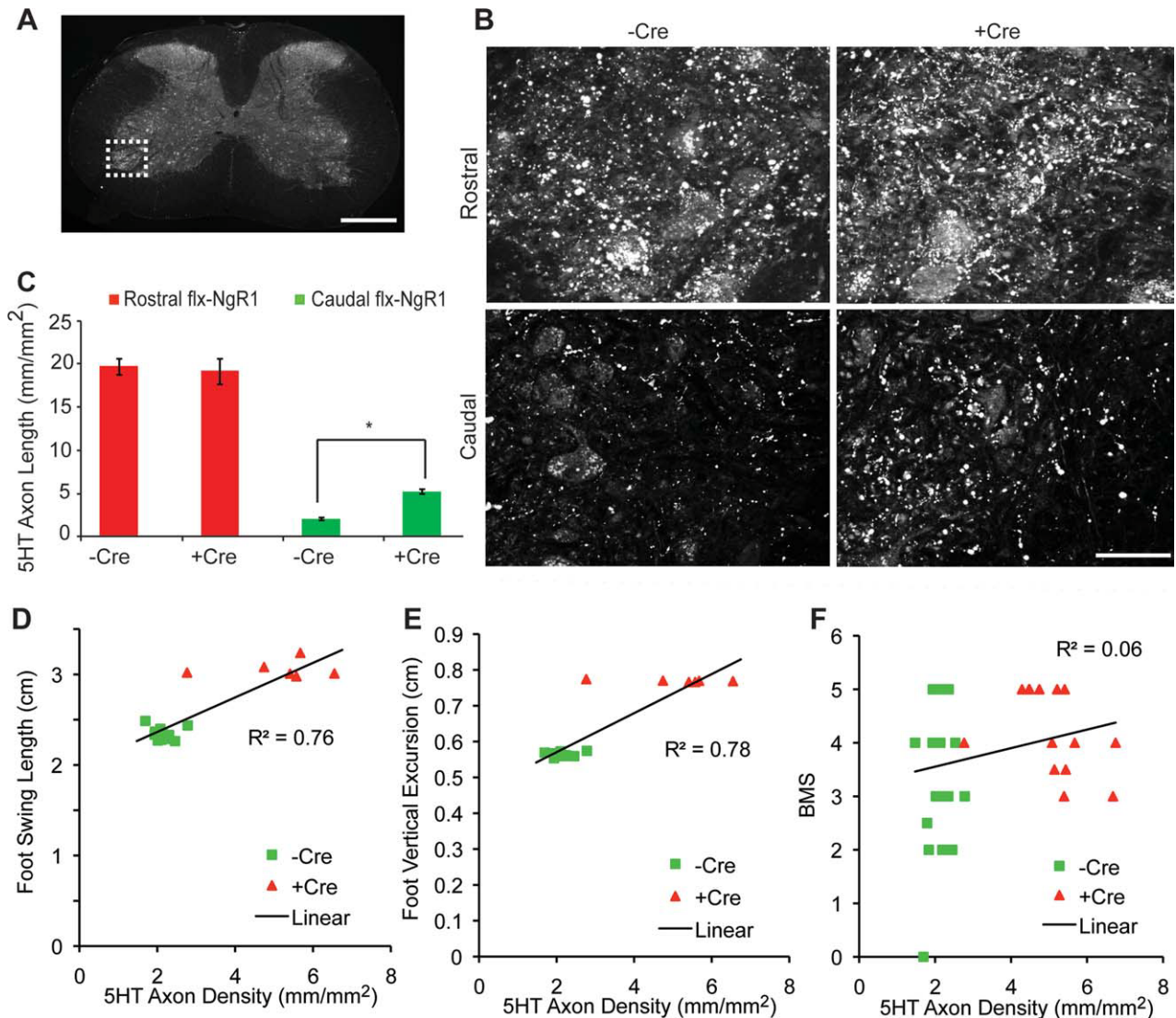


FIGURE 4: Raphespinal growth induced by NgR1 deletion in chronic spinal cord injury. (A) Low-magnification transverse section of the thoracic spinal cord indicates the ventral horn region shown at high magnification in B (dotted lines). Scale bar = 500 μ m. (B) Immunoreactive 5-hydroxytryptamine (5HT) fibers in the ventral horn of the cervical (rostral) and lumbar (caudal) enlargements are shown from a mouse with or without the Cre transgene following dorsal hemisection and tamoxifen treatment at 35 weeks after injury. Scale bar = 50 μ m. (C) The 5HT immunoreactive axonal length in B is shown. Data are mean \pm standard error of the mean, n = 23 mice for the Cre-negative and n = 18 mice for the Cre-positive group. * p < 0.01, 1-way analysis of variance with pairwise post hoc analysis using SPSS software. (D–F) Correlation coefficients from linear regression between 5HT immunoreactive axonal length and the kinematic analysis from Fig 3 or the Basso Mouse Scale (BMS) data from Fig 2 are shown. Correlation coefficients from linear regression are shown.

were not treated for 3 months, but hindlimb locomotor performance was evaluated weekly. The average BBB score at 12 weeks was 7.75 ± 0.10 , n = 64 (Fig 5A), meaning that the majority of rats were capable of hindlimb movement, but not weight support.^{47,52} After an intracerebroventricular (i.c.v.) cannula was introduced, rats were randomized to receive either AA-NgR(310)ecto-Fc or control IgG protein for 12 weeks at a dose of 0.29mg/kg/day^{21,37,38} (see Fig 4B). The initial BBB scores were identical in the 2 groups (see Fig 5). Twelve weeks later, there was a trend toward improved

hindlimb grip strength in rats treated with NgR1 decoy protein (hindlimb force as a percentage of forelimb force, $11.5 \pm 0.8\%$, n = 13 in IgG group assessed for grip strength vs $14.5 \pm 2.2\%$, n = 12 in NgR group; $p = 0.11$, 1-tailed t test). However, the more conspicuous behavioral change was the conversion from hindlimb non-weight-bearing to hindlimb weight-bearing locomotion. The number of AA-NgR(310)ecto-Fc-treated animals able to bear weight in the open field increased by 10 (29% of 35 rats, $p < 0.05$), whereas there was no significant increase in weight bearing in the control IgG group

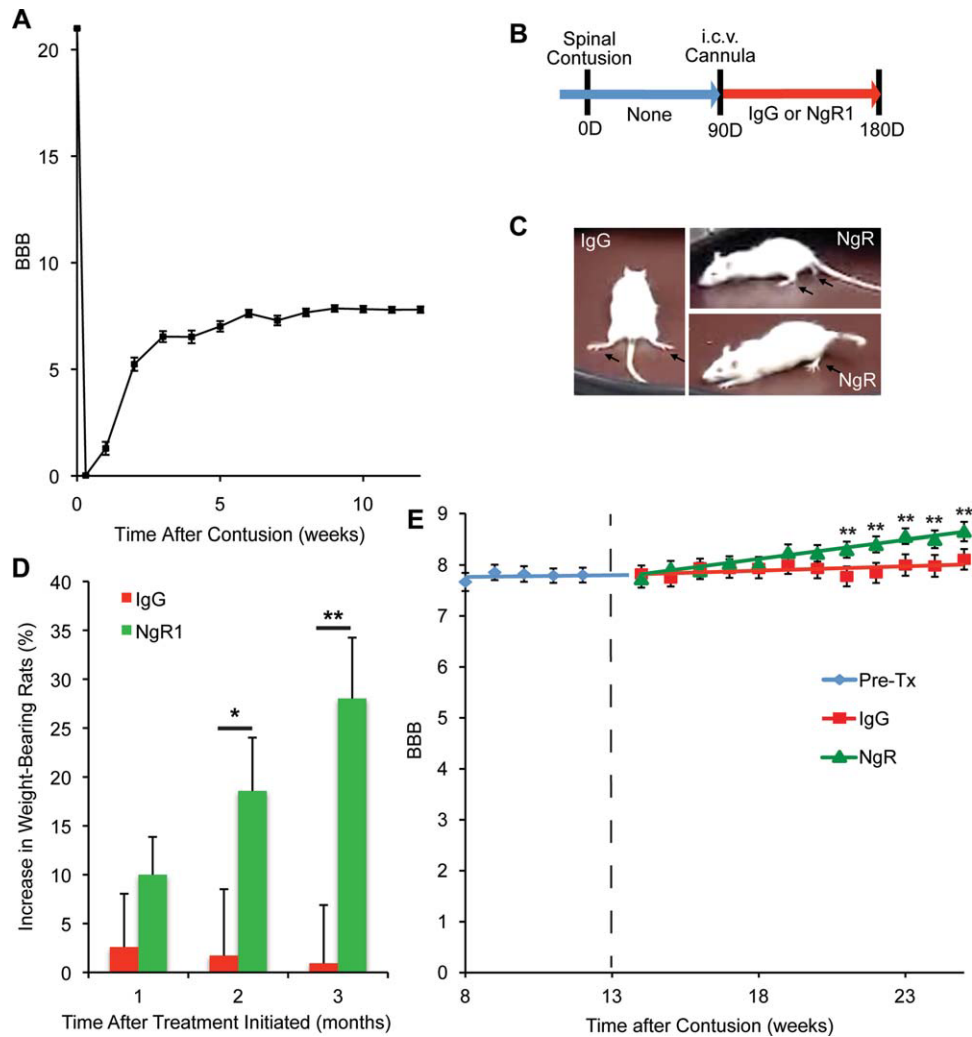


FIGURE 5: Recovery of weight bearing after NgR1 treatment of chronically spinal cord-contused rats. (A) Spontaneous improvement of open field locomotion (Basso, Beattie, and Bresnahan [BBB] score) as a function of time after thoracic spinal cord contusion injury for all rats prior to randomization to immunoglobulin G (IgG) or NgR1 treatment. Mean \pm standard error of the mean (SEM), $n = 64$. (B) Schematic of experiment. Two weeks after the intracerebroventricular (i.c.v.) cannula implantation (12 weeks after contusion injury), rats were assigned to 1 of 2 treatment groups. The phosphate-buffered saline (PBS) minipumps were replaced with new osmotic minipumps filled with 2.25mg AA-NgR(310)ecto-Fc (0.29mg/kg/day) or 2.25mg rat IgG in 2ml PBS. The duration of treatment was 12 weeks. A new osmotic minipump filled with the same amount of AA-NgR(310)ecto-Fc or rat IgG replaced each depleted pump every 4 weeks. (C) Examples of a control rat without weight support at the end of the treatment period and 2 of the 7 AA-NgR(310)ecto-Fc-treated rats that regained weight support. (D) The increase in the percentage of rats showing body weight support with at least 1 hindlimb as a function of time during therapy is reported. $p = 0.022$ by repeated measures analysis of variance (ANOVA) for the effect of NgR1 versus IgG treatment, and $*p < 0.05$ and $**p < 0.01$ for the indicated comparisons by 1-way ANOVA. (E) The course of recovery after the initiation of treatment (Tx) (dotted line) is plotted as a function of time. The locomotor BBB scores from the IgG and AA-NgR(310)ecto-Fc-treated groups were indistinguishable at the initiation of treatment. Data are mean \pm SEM, $n = 29$ for the IgG and $n = 35$ for the NgR1 group. $p = 0.002$ by repeated measures ANOVA for the effect of NgR1 versus IgG treatment, and $**p < 0.01$ by 1-way ANOVA for NgR1-treated values relative to pretreatment values by post hoc Fisher least-significant difference test using SPSS software.

(29 rats). During the treatment phase of the study, BBB scores showed a significant improvement in the NgR-treated group relative to the IgG group ($p = 0.002$ by repeated measures ANOVA), whereas no significant improvement versus time was detected in the IgG group from a pretreatment value of 7.75 ± 0.10 to 8.10 ± 0.20 post-treatment. BBB scores of the AA-

NgR(310)ecto-Fc-treated group were significantly improved between 8 and 12 weeks of treatment, at 21 to 25 weeks postcontusion ($p < 0.01$, ANOVA, from 7.75 ± 0.10 at 12 weeks to 8.65 ± 0.20 at 25 weeks). Thus, AA-NgR(310)ecto-Fc treatment of chronic spinal contusion improves neurological recovery, in particular open field locomotion.

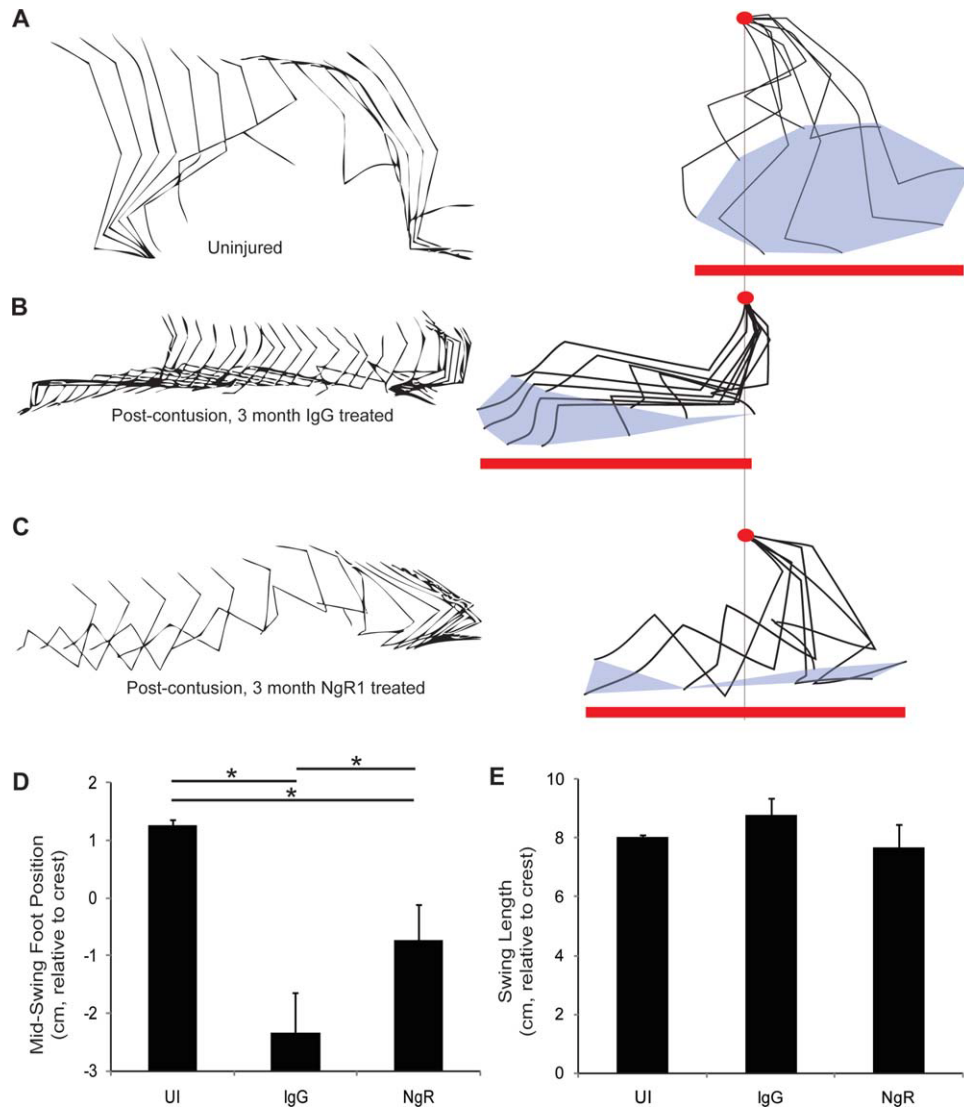


FIGURE 6: Gait kinematics in chronic spinal cord injury rats after NgR1 treatment. (A–C) Stick tracing of joint and limb position in the anterior–posterior plane (left), with forward to the right, and every 16th frame shown. The limb positions after normalizing to the iliac crest position (red dot) are provided at right. The total extent of foot swing (red line) and the toe cycle (shaded area) are shown. The individual examples are of an uninjured animal (A), and of rats after treatment for 12 weeks with immunoglobulin G (IgG) (B) or with AA-NgR(310)ecto-Fc (C). (D) The mid position of the foot swing relative to the iliac crest during the gait cycle in the different treatment groups. Data are mean \pm standard error of the mean (SEM) for $n = 12$ to 14 limbs per condition. UI = uninjured. $*p < 0.05$ by one-way ANOVA with post-hoc pairwise comparison, SPSS. (E) The anterior–posterior extent of foot movement relative to the iliac crest for the different treatment groups. Data are mean \pm SEM for $n = 12$ to 14 limbs per condition.

To provide quantitative measurements of open field locomotion, we also monitored limb kinematics in a randomly selected subset of control and AA-NgR(310)ecto-Fc-treated rats (Fig 6). In comparison to uninjured animals, the control group at 6 months after contusion injury exhibited multiple deficits. First, whereas the length of the foot swing in the anterior–posterior dimension on each step relative to the iliac crest was maintained at near normal levels, the average foot position was shifted far posterior. This observation is in agreement with a previous study.⁵⁹ Second, uninjured rats produced

a gait cycle in which the foot was centered under or anterior to the iliac crest, but the chronically contused control rats showed a range of foot position that remained posterior to the iliac crest at all times. In contrast, in the AA-NgR(310)ecto-Fc-treated group, there was significant normalization of foot position. The majority of AA-NgR(310)ecto-Fc-treated rats moved their foot anterior to the iliac crest with each cycle. The average position of the foot relative to the iliac crest resembled that of uninjured rats to a greater extent than it did the control injury group. The reproducibility of this result is

illustrated for 5 IgG protein-treated control and 5 AA-NgR(310)ecto-Fc-treated rats (Supplementary Fig S4). Ankle flexion of the AA-NgR(310)ecto-Fc-treated rats was confined significantly more precisely to the swing phase of the gait cycle than for the IgG-treated rats (Supplementary Fig S5). For the control IgG group, the ankle angle was extended 200 milliseconds prior to maximal foot movement and remained flexed for 200 milliseconds afterward. In this sense, the NgR-treated rats resembled uninjured rats more closely than did the control injury group.

In previous studies examining the potential benefit of NgR1 antagonism following SCI, improved neurological function correlated with axonal growth.^{16,18,20,21,37–39} Postmortem histological examination of rats treated after acute SCI with NgR(310)ecto-Fc revealed an increase in the density of descending raphespinal axons caudal to the lesion site.^{37,38} Similarly, here we observed increased 5HT fiber length in the lumbar spinal cord after treatment of chronic SCI (Fig 7A–F). Camera lucida reconstructions of sagittal sections of thoracic spinal cord illustrate increased 5HT-immunoreactive raphespinal fibers throughout the caudal spinal cord of AA-NgR(310)ecto-Fc-treated rats in comparison to IgG-treated controls (see Fig 7G, H). As expected, the degree of tissue loss at the injury site was not altered by AA-NgR(310)ecto-Fc treatment at this chronic stage (Supplementary Fig S6). Whereas there was a trend toward BDA-labeled corticospinal tract (CST) fibers extending into the lesion site, no CST fibers were detected in the spinal cord caudal to the lesion for either group (Supplementary Fig S7), consistent with findings in subacute treatment of rat contusion injury with NgR(310)ecto-Fc.³⁷ These data provide histological evidence for axon growth from uninjured and/or injured fibers as a mechanism contributing to the behavioral improvement of rats treated with AA-NgR(310)ecto-Fc at a chronic stage following spinal contusion.

Positron Emission Tomography Imaging of Raphespinal Growth after NgR1 Decoy Treatment of Chronic Rat Spinal Contusion

Proof of concept clinical trials for chronic SCI would be greatly enhanced by methods to directly monitor the presence of axonal growth noninvasively. Diffusion tensor imaging by magnetic resonance can detect massive disruptions of highly fascicular spinal cord tracts after injury, but it is extremely doubtful that this method can image the branched, tortuous, and disorganized growth of descending raphespinal fibers that occurs after SCI in response to AA-NgR(310)ecto-Fc treatment.^{14,16,18,20,21,37,38,60}

To visualize raphespinal axon growth in the caudal spinal cord in vivo, we evaluated imaging of presynaptic serotonin reuptake sites by PET. One ligand, [¹¹C]AFM, shows highly selective binding to serotonin transporters (SERT, 5HTT) in vivo.^{55,56} To verify the feasibility of such a PET ligand for use in detecting changes after spinal contusion, we first examined 5HTT immunoreactivity in sagittal sections from injured animals and compared these results to our findings with 5HT immunostaining for raphespinal fibers. We observed an increase in 5HTT fiber length in the caudal spinal cord of NgR(310)ecto-Fc-treated rats that was very similar to the distribution of 5HT-immunolabeled fibers (see Fig 7). Therefore, we obtained PET images from the spinal cord of anesthetized rats. The [¹¹C]AFM tracer exhibits high uptake in the brain and spinal cord at 30 to 60 minutes postinjection. The fraction of [¹¹C]AFM activity uptake attributable to nonspecific binding was determined by blockade with the competitive 5HTT inhibitor citalopram in healthy control animals. The ratio of standard uptake values (concentration normalized by activity dose and body weight) between citalopram and baseline scans was 0.35 ± 0.05 and 0.33 ± 0.05 for the cervical and lumbar cord, respectively (mean \pm standard error of the mean, $n = 5$), that is, $>70\%$ of the uptake at 30 to 60 minutes is specific binding. The nonspecific uptake fraction (30%) was then used to correct the total uptake values to specific uptake values. In rats with thoracic spinal cord complete transection, the cervical [¹¹C]AFM-specific binding signal is similar to that in uninjured animals, but the signal in the lumbar enlargement is eliminated.

For spinal contusion rats prior to treatment at 3 months postinjury, an 80% reduction deficit in lumbar cord [¹¹C]AFM-specific signal is detected relative to cervical values (see Fig 7O–P). After treatment with NgR(310)ecto-Fc for 3 months, the lumbar specific uptake as a proportion of the cervical uptake was 2-fold greater than in IgG-treated rats or in pretreatment rats ($p < 0.05$, ANOVA; see Fig 7O–P), matching immunohistological results with either 5HT or 5HTT (see Fig 7I, J). Thus, PET imaging of 5HTT with [¹¹C]AFM provides a noninvasive method to monitor serotonergic axonal growth after treatment with the axonal growth-promoting compound AA-NgR(310)ecto-Fc.

Discussion

The major finding of the present work is that axon growth and neurological improvement can be achieved with a single molecular intervention in the chronically injured adult CNS. We utilized 2 different interventions

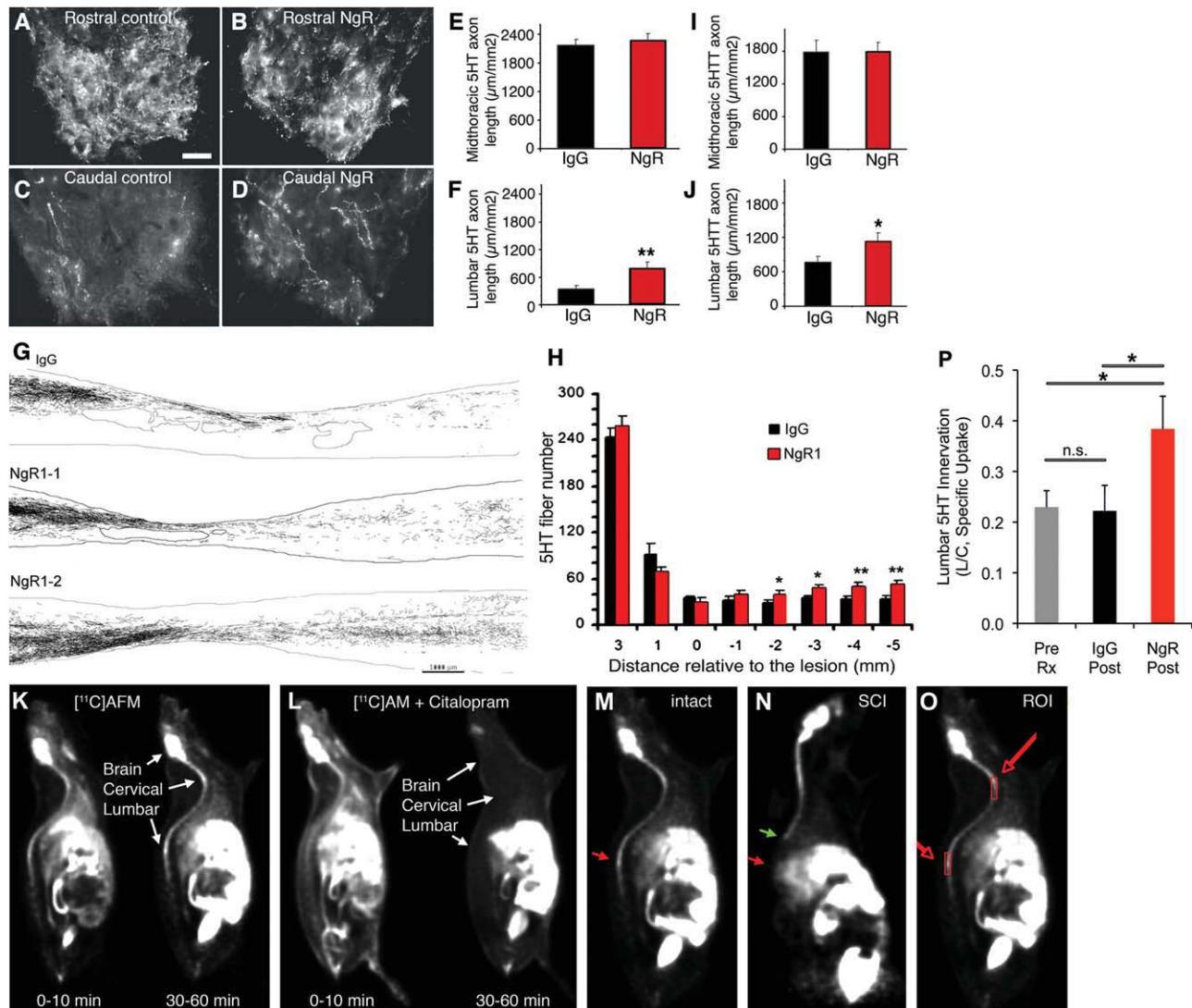


FIGURE 7: AA-NgR(310)ecto-Fc-induced raphespinal growth in chronic spinal cord injury (SCI). (A–D) Transverse sections from the spinal cord 11 to 15mm rostral or caudal to the contusion site were immunostained as indicated from rats completing 3 months of intracerebroventricular treatment. Antiserotonin immunohistochemistry labels 5-hydroxytryptamine (5HT) fibers in the ventral horn of the spinal cord. Note the decreased innervation caudal to the injury and the partial recovery in the AA-NgR(310)ecto-Fc-treated rats. Scale bar = 25 μ m. (E, F) The length of 5HT-immunoreactive axon per unit area of ventral horn in the transverse plane was measured for chronic SCI rats completing 3 months treatment with the indicated proteins from micrographs as in A–D. The data are mean \pm standard error of the mean (SEM) for n = 21 to 25 per group, and the increase in the NgR1-treated group in the distal cord is significant; ** p < 0.01, analysis of variance (ANOVA). (G) Camera lucida drawings of serotonergic fibers from 1 immunoglobulin G (IgG)-treated and 2 AA-NgR(310)ecto-Fc-treated animals. Each drawing is a composite assembled from a set of 10 parasagittal sections spaced at intervals of 200 μ m across the spinal cord. The contusion cavities are encircled near the center of each image. Increased numbers of serotonergic fibers are observed in the caudal spinal cord in the AA-NgR(310)ecto-Fc-treated (NgR1-1, NgR1-2) animals compared with the IgG-treated animals. Scale bar = 1,000 μ m. (H) 5HT fiber number at various distances rostral and caudal to the center of the lesion from AA-NgR(310)ecto-Fc-treated (red bars) and control animals (black bars) is reported. * p < 0.05, ** p < 0.01, ANOVA. For the x-axis, a positive value is rostral to the center of the lesion, and a negative value is caudal to the center of lesion. (I, J) Adjacent sections were processed for antiserotonin transporter (5HTT) immunohistochemistry and measured as for 5HT in E, F. The data are mean \pm SEM for n = 21 to 25 per group, and the increase in the NgR1 group in the distal cord is significant, * p < 0.05, ANOVA. (K, L) [11 C]AFM radioactivity was visualized at the indicated times after an intravenous injection of tracer (50 \pm 30MBq, 0.12 \pm 0.09 μ g) with or without the preinjection of the competitive ligand, citalopram (2mg/kg, 15 minutes before [11 C]AFM injection). The initial distribution of the tracer is broad with or without citalopram at 0 to 10 minutes. Specific uptake of [11 C]AFM at 30 to 60 minutes in the brain, cervical spinal cord, and lumbar spinal cord is blocked by citalopram. (M, N) A rat with an intact spinal cord was imaged with [11 C]AFM and compared to a rat with a midthoracic transection 1 week earlier. Uptake at 30 to 60 minutes is illustrated. The site of the lesion is indicated by the green arrow, and the reduced uptake in the lumbar cord of the injured rat is indicated by the red arrow. (O) For quantitation of [11 C]AFM uptake in the spinal cord, 2 regions of interest (ROIs) were selected as illustrated by the boxes on this intact rat image. (P) The ratio of lumbar to cervical (L/C) [11 C]AFM specific uptake at 30 to 60 minutes post-tracer injection was determined in injured rats completing 3 months of treatment with control IgG or NgR(310)ecto-Fc, as illustrated in O. The data are mean \pm SEM for n = 21 to 23 per group, and the increase in the NgR1 group in the distal cord is significant; * p < 0.05, ANOVA. n.s. = not significant; Rx = treatment.

in 2 different SCI model systems to verify that NgR1-directed intervention is effective many months after thoracic SCI. In mice, we generated a conditional allele of NgR1 and employed a drug-regulated Cre-dependent deletion strategy to study the role of NgR1 in limiting recovery at a chronic stage following dorsal hemisection SCI. In rats, we utilized intracerebral infusion to evaluate the effects of an NgR1 decoy receptor at a chronic stage after contusion SCI. In both systems, months after thoracic injury, intervention significantly improved open field locomotion, hindlimb kinematics, and caudal raphespinal axon density. These data provide the first demonstration that a directed molecular intervention has preclinical efficacy for improving mammalian neurological function in the chronic stage of CNS damage.

In previous analyses of chronic SCI, cell-based combination therapies have yielded some benefit. Cellular components have included olfactory ensheathing cells, Schwann cells, fibroblasts, neural stem cells, and mesenchymal stem cells.^{10–12} To achieve optimal benefits, cellular transplantation has been combined with a range of interventions, including modifications of cyclic adenosine monophosphate (cAMP) level, surgeries to promote the intrinsic growth stage of the neuron, and neurotrophic factors. None of these interventions has produced significant neurological benefit for chronic SCI in the absence of surgical transplantation. In contrast to chronic SCI, several pharmacological treatments without surgical or cell-based intervention are beneficial in acute or subacute models of SCI. Pharmacological treatments targeting myelin-derived inhibitors, chondroitin sulfate proteoglycans, intracellular RhoA signaling cascades, cAMP levels, and neurotrophic factors are efficacious when employed shortly after injury.⁴ Similar to pharmacological intervention, perturbing the expression of single genes to promote axon growth and/or neurological improvement, including PTEN (phosphatase and tensin homolog),⁶¹ Nogo-A,^{7,8,14,15,18} NgR1,²⁰ and PTP-sigma,^{62,63} has only been effective when performed before or shortly after SCI. The current study establishes the possibility of pharmacological therapy alone as efficacious for chronic CNS injuries such as spinal cord trauma.

The locomotor and kinematic improvements observed in chronically injured mice and rats after NgR1 perturbation emerge gradually and correlate with increased serotonin fiber density in the distal spinal cord. Most likely this reflects sprouting of raphespinal fibers. Treatment with the NgR1 decoy protein did not promote long-distance regeneration of corticospinal fibers in the rat chronic contusion model. However, many lines of work support the model that short-range anatomical plasticity such as collateral sprouting can provide substantial

functional benefit in the absence of long-distance axon regeneration. For example, the sprouting of uninjured corticospinal fibers after pyramidotomy and after ischemic stroke in constitutive mutant NgR1 mice correlates with functional recovery in the absence of regeneration.^{15,21} This restitution of function may depend in part on the recruitment of intraspinal polysynaptic relays capable of providing substantial neurological replacement for injured long tracts.^{5,64} Thus, an absence of frank corticospinal regeneration does not imply absent restoration of functional polysynaptic circuits. Pharmacological interventions, such as ibuprofen and Y-27632, also promote axonal sprouting and functional recovery after SCI without long distance axonal regeneration.^{41,65} Although the growth of raphespinal serotonin axons in the caudal spinal cord is driven by NgR1 intervention long after SCI, anatomical rearrangements of other injured and uninjured descending and propriospinal fiber tracts at multiple levels of neuraxis are probable contributors to the improvements in locomotion and kinematics observed in this study.

Although sprouting or plasticity are likely to occur with interruption of NgR1 pathways, the optic nerve regeneration studies with constitutive or conditional NgR1 deletion demonstrate that absence of this 1 protein in adult mice permits axonal regeneration per se in vivo. This finding extends previous studies using a dominant negative truncated NgR1 virus in combination with an induction of intrinsic growth potential by macrophage inflammation.⁴⁶ Presumably, the more prominent phenotype after genetic deletion reflects incomplete infection with the dominant negative virus coupled with incomplete blockade in the face of continued expression of endogenous NgR1.

As NgR1 intervention permits axonal sprouting and functional improvement long after injury, myelin inhibitors may be continuously suppressing CNS rewiring by stabilizing CNS anatomy. This function of myelin-associated inhibitors and NgR1 is consistent with the finding that NgR1 is required to restrict ocular dominance plasticity in the visual system to a developmental critical period. Adult NgR1 mutant mice preserve this experience-dependent plasticity at a level indistinguishable from adolescent critical period mice.⁶⁶ Thus, myelin and NgR1 may contribute to consolidating neural circuitry and the efficacy of myelin neutralization to support functional improvement after chronic injury derives from the continuous physiologic role of myelin of dampening anatomical rearrangements at the synaptic level.

Acute blockade of NgR1 function within several days of spinal cord contusion improves locomotor recovery, with an average of a 2.75-point improvement on the

BBB scale and 2-fold increase in the occurrence of weight-bearing status.⁶⁷ The time dependence of benefits from NgR decoy treatment is difficult without direct comparison in the same experiment. However, the benefit for chronic injury appears to be of lesser magnitude than for treatment initiated within a week of contusion. This suggests that NgR1-independent factors allow the recently injured nervous system to more fully capitalize on a growth environment rendered more conducive to growth by NgR1 blockade.

The open field BMS and BBB scoring systems have played a key role in the analysis of motor dysfunction after SCI. Limb kinematic analysis is more detailed and provides additional insights into motor performance.^{5,59,68,69} Although the use of these systems is increasing, much of the work has been restricted to body weight-supported treadmill stepping. Its use for spontaneous locomotion has been limited. Thus, baseline data for moderately injured mice and rats have few precedents in the literature. The strong correlation between recovery of raphespinal innervation in the lumbar spinal cord and kinematic parameters is consistent with fiber growth mediating return of function.

The type of movement impairment in mice with a chronic dorsal hemisection is distinct from that in rats with a moderate spinal contusion. Chronically injured mice exhibited shortened swing of the foot relative to the hip. In agreement with previous short-term studies,⁵⁹ we observed a pronounced effect on limb position in chronically injured rats. The foot was maintained in a posterior position despite relatively preserved anterior–posterior excursions with each gait cycle relative to the iliac crest. The use of such analysis in a broader range of studies is likely to provide greater insight into the mechanisms and pathways of recovery. In the current study, NgR1 intervention improved limb kinematics to more closely resemble the uninjured state despite treatment being initiated 2 months after injury.

Among the parameters derived from kinematic analysis are joint angles. However, the interpretation of such angles in cases of significant dysfunction without assisted stepping is not straightforward. We observed greater ankle angles through the gait cycle in mice with NgR1 deletion. This is consistent with greater strength and weight support, but it might reflect changes in posture or tone rather than strength or coordination. For the spinal contused rats, most animals were not weight-supporting, and full ankle extension/flexion during sweeping gait cycles of the externally rotated hindlimb on the floor were noted. In the NgR-treated rats, ankle angles were linked with greater temporal precision to the gait cycle than in untreated rats. Moreover, the NgR-

treated pattern more closely resembled the uninjured ankle angle pattern.

The translation of laboratory findings to clinical studies is strongly facilitated by quantitative biomarkers that monitor the primary mechanism of action. For SCI, functional analysis at the bedside using clinical scores has been the mainstay of analysis.⁷⁰ Electrophysiological analysis may provide additional confirmatory measurements, but these have seldom been used clinically or in injury models. To date, magnetic resonance imaging (MRI) studies have been used primarily to define the extent of injury rather than a degree of sprouting, plasticity, repair, or recovery. Although the blood oxygenation level-dependent signal in functional MRI studies and the diffusion tensor method may provide additional insights, they cannot be considered biomarkers for the action of axon growth promoters.⁷¹ Because our anatomical studies demonstrated highly branched sprouting of serotonergic fibers in the lumbar spinal cord, we sought a translatable method to monitor this growth. PET with serotonin transporter ligands provides a method to monitor the action of these interventions that drive neurological recovery and axon growth.

Our observation that chronically injured animals can regain neurological function following administration of a single pharmacological reagent has 2 important implications. First, these findings demonstrate that at least 1 axon growth-promoting therapy may have relevance for pre-existing spinal cord trauma. Second, these results may facilitate translational research, because clinical trials of therapies for chronic spinal cord damage can be powered adequately with <10% of the number of patients required for acute therapies.⁷² In conclusion, perturbation of NgR1 pathways supports recovery of neurological function in chronic rodent SCI.

Acknowledgments

A.W.M. holds a Career Award in the Biomedical Sciences from the Burroughs Wellcome Fund. This work was supported by grants from the Christopher and Dana Reeve Foundation, the Wings for Life Foundation, and the Dr Ralph and Marion Falk Medical Research Trust to S.M.S., and from the NINDS to N.Y.H., L.I.B., W.B.J.C., and S.M.S.

We thank Y. Fu and the Yale PET Center staff for outstanding technical assistance, and Biogen Idec Inc. for providing NgR-Fc fusion protein.

Authorship

X.W., P.D., and A.W.M. contributed equally to the study.

Potential Conflicts of Interest

S.M.S.: grants/grants pending, Biogen Idec, Axerion Therapeutics; consulting fees, Biogen Idec; patents, Axerion Therapeutics; royalties, Axerion Therapeutics; stock/stock options, Axerion Therapeutics; cofounder of Axerion Therapeutics, which seeks to develop PrP and NgR therapies.

References

- Rossignol S, Schwab M, Schwartz M, Fehlings MG. Spinal cord injury: time to move? *J Neurosci* 2007;27:11782–11792.
- Liu BP, Cafferty WB, Budel SO, Strittmatter SM. Extracellular regulators of axonal growth in the adult central nervous system. *Philos Trans R Soc Lond B Biol Sci* 2006;361:1593–1610.
- Maier IC, Schwab ME. Sprouting, regeneration and circuit formation in the injured spinal cord: factors and activity. *Philos Trans R Soc Lond B Biol Sci* 2006;361:1611–1634.
- Bradbury EJ, McMahon SB. Spinal cord repair strategies: why do they work? *Nat Rev Neurosci* 2006;7:644–653.
- Courtine G, Song B, Roy RR, et al. Recovery of supraspinal control of stepping via indirect propriospinal relay connections after spinal cord injury. *Nat Med* 2008;14:69–74.
- Rosenzweig ES, Courtine G, Jindrich DL, et al. Extensive spontaneous plasticity of corticospinal projections after primate spinal cord injury. *Nat Neurosci* 2010;13:1505–1510.
- Cafferty WB, Duffy P, Huebner E, Strittmatter SM. MAG and OMgp synergize with Nogo-A to restrict axonal growth and neurological recovery after spinal cord trauma. *J Neurosci* 2010;30:6825–6837.
- Cafferty WB, McGee AW, Strittmatter SM. Axonal growth therapeutics: regeneration or sprouting or plasticity? *Trends Neurosci* 2008;31:215–220.
- Spinal cord injury, facts and figures at a glance. Birmingham, AL: National Spinal Cord Injury Statistical Center, 2006.
- Kadoya K, Tsukada S, Lu P, et al. Combined intrinsic and extrinsic neuronal mechanisms facilitate bridging axonal regeneration one year after spinal cord injury. *Neuron* 2009;64:165–172.
- Karimi-Abdolrezaee S, Eftekharpour E, Wang J, et al. Synergistic effects of transplanted adult neural stem/progenitor cells, chondroitinase, and growth factors promote functional repair and plasticity of the chronically injured spinal cord. *J Neurosci* 2010;30:1657–1676.
- Tom VJ, Sandrow-Feinberg HR, Miller K, et al. Combining peripheral nerve grafts and chondroitinase promotes functional axonal regeneration in the chronically injured spinal cord. *J Neurosci* 2009;29:14881–14890.
- Fournier AE, GrandPre T, Strittmatter SM. Identification of a receptor mediating Nogo-66 inhibition of axonal regeneration. *Nature* 2001;409:341–346.
- Dimou L, Schnell L, Montani L, et al. Nogo-A-deficient mice reveal strain-dependent differences in axonal regeneration. *J Neurosci* 2006;26:5591–5603.
- Cafferty WB, Strittmatter SM. The Nogo-Nogo receptor pathway limits a spectrum of adult CNS axonal growth. *J Neurosci* 2006;26:12242–12250.
- Cafferty WB, Kim JE, Lee JK, Strittmatter SM. Response to correspondence: Kim et al., “Axon regeneration in young adult mice lacking Nogo-A/B.” *Neuron* 38, 187–199. *Neuron* 2007;54:195–199.
- Lee JK, Geoffroy CG, Chan AF, et al. Assessing spinal axon regeneration and sprouting in Nogo-, MAG-, and OMgp-deficient mice. *Neuron* 2010;66:663–670.
- Kim JE, Li S, GrandPre T, et al. Axon regeneration in young adult mice lacking Nogo-A/B. *Neuron* 2003;38:187–199.
- Simonen M, Pedersen V, Weinmann O, et al. Systemic deletion of the myelin-associated outgrowth inhibitor Nogo-A improves regenerative and plastic responses after spinal cord injury. *Neuron* 2003;38:201–211.
- Kim JE, Liu BP, Park JH, Strittmatter SM. Nogo-66 receptor prevents raphespinal and rubrospinal axon regeneration and limits functional recovery from spinal cord injury. *Neuron* 2004;44:439–451.
- Lee JK, Kim JE, Sivula M, Strittmatter SM. Nogo receptor antagonism promotes stroke recovery by enhancing axonal plasticity. *J Neurosci* 2004;24:6209–6217.
- Zheng B, Atwal J, Ho C, et al. Genetic deletion of the Nogo receptor does not reduce neurite inhibition in vitro or promote corticospinal tract regeneration in vivo. *Proc Natl Acad Sci U S A* 2005;102:1205–1210.
- Atwal JK, Pinkston-Gosse J, Syken J, et al. PirB is a functional receptor for myelin inhibitors of axonal regeneration. *Science* 2008;322:967–970.
- Omoto S, Ueno M, Mochio S, et al. Genetic deletion of paired immunoglobulin-like receptor B does not promote axonal plasticity or functional recovery after traumatic brain injury. *J Neurosci* 2010;30:13045–13052.
- Nakamura Y, Fujita Y, Ueno M, et al. Paired immunoglobulin-like receptor B knockout does not enhance axonal regeneration or locomotor recovery after spinal cord injury. *J Biol Chem* 2011;286:1876–1883.
- Liebscher T, Schnell L, Schnell D, et al. Nogo-A antibody improves regeneration and locomotion of spinal cord-injured rats. *Ann Neurol* 2005;58:706–719.
- Wiessner C, Bareyre FM, Allegrini PR, et al. Anti-Nogo-A antibody infusion 24 hours after experimental stroke improved behavioral outcome and corticospinal plasticity in normotensive and spontaneously hypertensive rats. *J Cereb Blood Flow Metab* 2003;23:154–165.
- Freund P, Schmidlin E, Wannier T, et al. Nogo-A-specific antibody treatment enhances sprouting and functional recovery after cervical lesion in adult primates. *Nat Med* 2006;12:790–792.
- Zomer B, Schwab ME. Anti-Nogo on the go: from animal models to a clinical trial. *Ann N Y Acad Sci* 2010;1198(suppl 1):E22–E34.
- GrandPre T, Li S, Strittmatter SM. Nogo-66 receptor antagonist peptide promotes axonal regeneration. *Nature* 2002;417:547–551.
- Li S, Strittmatter SM. Delayed systemic Nogo-66 receptor antagonist promotes recovery from spinal cord injury. *J Neurosci* 2003;23:4219–4227.
- Cao Y, Shumsky JS, Sabol MA, et al. Nogo-66 receptor antagonist peptide (NEP1-40) administration promotes functional recovery and axonal growth after lateral funiculus injury in the adult rat. *Neurorehabil Neural Repair* 2008;22:262–278.
- Fang PC, Barbay S, Plautz EJ, et al. Combination of NEP 1-40 treatment and motor training enhances behavioral recovery after a focal cortical infarct in rats. *Stroke* 2010;41:544–549.
- Zai L, Ferrari C, Dice C, et al. Inosine augments the effects of a Nogo receptor blocker and of environmental enrichment to restore skilled forelimb use after stroke. *J Neurosci* 2011;31:5977–5988.
- Steward O, Sharp K, Yee KM, Hofstadter M. A re-assessment of the effects of a Nogo-66 receptor antagonist on regenerative growth of axons and locomotor recovery after spinal cord injury in mice. *Exp Neurol* 2008;209:446–468.

36. Fournier AE, Gould GC, Liu BP, Strittmatter SM. Truncated soluble Nogo receptor binds Nogo-66 and blocks inhibition of axon growth by myelin. *J Neurosci* 2002;22:8876–8883.
37. Wang X, Baughman KW, Basso DM, Strittmatter SM. Delayed Nogo receptor therapy improves recovery from spinal cord contusion. *Ann Neurol* 2006;60:540–549.
38. Li S, Liu BP, Budel S, et al. Blockade of nogo-66, myelin-associated glycoprotein, and oligodendrocyte myelin glycoprotein by soluble nogo-66 receptor promotes axonal sprouting and recovery after spinal injury. *J Neurosci* 2004;24:10511–10520.
39. Harvey PA, Lee DH, Qian F, et al. Blockade of Nogo receptor ligands promotes functional regeneration of sensory axons after dorsal root crush. *J Neurosci* 2009;29:6285–6295.
40. Duffy P, Schmandke A, Sigworth J, et al. Rho-associated kinase II (ROCKII) limits axonal growth after trauma within the adult mouse spinal cord. *J Neurosci* 2009;29:15266–15276.
41. Fournier AE, Takizawa BT, Strittmatter SM. Rho kinase inhibition enhances axonal regeneration in the injured CNS. *J Neurosci* 2003;23:1416–1423.
42. Dergham P, Ellezam B, Essagian C, et al. Rho signaling pathway targeted to promote spinal cord repair. *J Neurosci* 2002;22:6570–6577.
43. Lehmann M, Fournier A, Selles-Navarro I, et al. Inactivation of Rho signaling pathway promotes CNS axon regeneration. *J Neurosci* 1999;19:7537–7547.
44. Jin Z, Strittmatter SM. Rac1 mediates collapsin-1-induced growth cone collapse. *J Neurosci* 1997;17:6256–6263.
45. Hayashi S, McMahon AP. Efficient recombination in diverse tissues by a tamoxifen-inducible form of Cre: a tool for temporally regulated gene activation/inactivation in the mouse. *Dev Biol* 2002;244:305–318.
46. Fischer D, He Z, Benowitz LI. Counteracting the Nogo receptor enhances optic nerve regeneration if retinal ganglion cells are in an active growth state. *J Neurosci* 2004;24:1646–1651.
47. Basso DM, Beattie MS, Bresnahan JC, et al. MASCIS evaluation of open field locomotor scores: effects of experience and teamwork on reliability. Multicenter Animal Spinal Cord Injury Study. *J Neurotrauma* 1996;13:343–359.
48. Young W. Spinal cord contusion models. *Prog Brain Res* 2002;137:231–255.
49. Park JH, Gimbel DA, GrandPre T, et al. Alzheimer precursor protein interaction with the Nogo-66 receptor reduces amyloid-beta plaque deposition. *J Neurosci* 2006;26:1386–1395.
50. Weinreb PH, Wen D, Qian F, et al. Resolution of disulfide heterogeneity in Nogo receptor I fusion proteins by molecular engineering. *Biotechnol Appl Biochem* 2010;57:31–45.
51. Basso DM, Fisher LC, Anderson AJ, et al. Basso Mouse Scale for locomotion detects differences in recovery after spinal cord injury in five common mouse strains. *J Neurotrauma* 2006;23:635–659.
52. Basso DM, Beattie MS, Bresnahan JC. A sensitive and reliable locomotor rating scale for open field testing in rats. *J Neurotrauma* 1995;12:1–21.
53. Cafferty WB, Yang SH, Duffy PJ, et al. Functional axonal regeneration through astrocytic scar genetically modified to digest chondroitin sulfate proteoglycans. *J Neurosci* 2007;27:2176–2185.
54. Li S, Kim JE, Budel S, et al. Transgenic inhibition of Nogo-66 receptor function allows axonal sprouting and improved locomotion after spinal injury. *Mol Cell Neurosci* 2005;29:26–39.
55. Williams WA, Neumeister A, Nabulsi N, et al. First in human evaluation of [¹¹C]AFM, a novel PET tracer for the serotonin transporter. *Neuroimage* 2008;41:T42.
56. Huang Y, Hwang DR, Bae SA, et al. A new positron emission tomography imaging agent for the serotonin transporter: synthesis, pharmacological characterization, and kinetic analysis of [¹¹C]-2-[2-(dimethylaminomethyl)phenylthio]-5-fluoromethylphenylamine ([¹¹C]AFM). *Nucl Med Biol* 2004;31:543–556.
57. Villegas-Perez MP, Vidal-Sanz M, Rasminsky M, et al. Rapid and protracted phases of retinal ganglion cell loss follow axotomy in the optic nerve of adult rats. *J Neurobiol* 1993;24:23–36.
58. Berkelaar M, Clarke DB, Wang YC, et al. Axotomy results in delayed death and apoptosis of retinal ganglion cells in adult rats. *J Neurosci* 1994;14:4368–4374.
59. Collazos-Castro JE, Lopez-Dolado E, Nieto-Sampedro M. Locomotor deficits and adaptive mechanisms after thoracic spinal cord contusion in the adult rat. *J Neurotrauma* 2006;23:1–17.
60. GrandPre T, Nakamura F, Vartanian T, Strittmatter SM. Identification of the Nogo inhibitor of axon regeneration as a Reticulon protein. *Nature* 2000;403:439–444.
61. Liu K, Lu Y, Lee JK, et al. PTEN deletion enhances the regenerative ability of adult corticospinal neurons. *Nat Neurosci* 2010;13:1075–1081.
62. Fry EJ, Chagnon MJ, Lopez-Vales R, et al. Corticospinal tract regeneration after spinal cord injury in receptor protein tyrosine phosphatase sigma deficient mice. *Glia* 2010;58:423–433.
63. Shen Y, Tenney AP, Busch SA, et al. PTPsigma is a receptor for chondroitin sulfate proteoglycan, an inhibitor of neural regeneration. *Science* 2009;326:592–596.
64. Bareyre FM, Kerschensteiner M, Raineteau O, et al. The injured spinal cord spontaneously forms a new intraspinal circuit in adult rats. *Nat Neurosci* 2004;7:269–277.
65. Wang X, Budel S, Baughman K, et al. Ibuprofen enhances recovery from spinal cord injury by limiting tissue loss and stimulating axonal growth. *J Neurotrauma* 2009;26:81–95.
66. McGee AW, Yang Y, Fischer QS, et al. Experience-driven plasticity of visual cortex limited by myelin and Nogo receptor. *Science* 2005;309:2222–2226.
67. Wang X, Baughman KW, Basso DM, Strittmatter SM. Delayed Nogo receptor therapy improves recovery from spinal cord contusion. *Ann Neurol* 2006;60:540–549.
68. Nessler JA, De Leon RD, Sharp K, et al. Robotic gait analysis of bipedal treadmill stepping by spinal contused rats: characterization of intrinsic recovery and comparison with BBB. *J Neurotrauma* 2006;23:882–896.
69. Pereira JE, Cabrita AM, Filipe VM, et al. A comparison analysis of hindlimb kinematics during overground and treadmill locomotion in rats. *Behav Brain Res* 2006;172:212–218.
70. Steeves JD, Lammertse D, Curt A, et al. Guidelines for the conduct of clinical trials for spinal cord injury (SCI) as developed by the ICCP panel: clinical trial outcome measures. *Spinal Cord* 2007;45:206–221.
71. Harel NY, Strittmatter SM. Functional MRI and other non-invasive imaging technologies: providing visual biomarkers for spinal cord structure and function after injury. *Exp Neurol* 2008;211:324–328.
72. Fawcett JW, Curt A, Steeves JD, et al. Guidelines for the conduct of clinical trials for spinal cord injury as developed by the ICCP panel: spontaneous recovery after spinal cord injury and statistical power needed for therapeutic clinical trials. *Spinal Cord* 2007;45:190–205.